

Raman modes of metallic carbon nanotubes

M. A. Pimenta* and A. Marucci

Department of Physics, Massachusetts Institute of Technology, Cambridge, Massachusetts 02139

S. A. Empedocles and M. G. Bawendi

Department of Chemistry, Massachusetts Institute of Technology, Cambridge, Massachusetts 02139

E. B. Hanlon

George R. Harrison Spectroscopy Laboratory, Massachusetts Institute of Technology, Cambridge, Massachusetts 02139

A. M. Rao and P. C. Eklund

Department of Physics and Astronomy, and Center for Applied Energy Research, University of Kentucky, Lexington, Kentucky 40506

R. E. Smalley

Department of Chemistry, Rice University, Houston, Texas 77005

G. Dresselhaus

Francis Bitter Magnet Laboratory, Massachusetts Institute of Technology, Cambridge, Massachusetts 02139

M. S. Dresselhaus

*Department of Physics, Massachusetts Institute of Technology, Cambridge, Massachusetts 02139
and Department of Electrical Engineering and Computer Science, Massachusetts Institute of Technology,
Cambridge, Massachusetts 02139*

(Received 22 September 1998)

The anomalous resonant behavior of the tangential Raman modes of carbon nanotubes has been studied in the critical region of laser energies 1.7–2.2 eV. The special enhancement of the Raman modes is explained by a model that takes into account the transition between the singularities in the one-dimensional density of electronic states for the *metallic* nanotubes and the distribution of diameters in the sample. The results agree with direct measurements of the electronic density of states for the metallic nanotubes and establish their association with the specially enhanced high frequency, first-order Raman modes. [S0163-1829(98)50848-X]

Resonant Raman spectroscopy is a very useful tool for the characterization of the one-dimensional (1D) properties of carbon nanotubes. It has been used to study multiwall nanotubes (MWNT),¹ single-wall nanotubes (SWNT),^{2–5} and was recently examined theoretically.⁶ We show here evidence that special tangential phonon modes of metallic carbon nanotubes are enhanced in a narrow range of laser energies between 1.7 and 2.2 eV by electronic transitions between the first singularities in the 1D electronic density of states (DOS) in the valence and conduction bands $v_1 \rightarrow c_1$. This result establishes the association of the specially enhanced high-frequency, tangential modes with the *metallic* carbon nanotubes.

The unique resonant behavior of the Raman spectra in SWNTs was first reported by Rao *et al.*,² who showed that the shape and position of the Raman bands associated with the radial breathing mode (RBM), around 180 cm^{-1} were strongly dependent on the energy of the exciting laser E_{laser} . This result was identified² with the tube diameter dependence of both the RBM frequency and the separation between the singularities in the valence and conduction bands of the 1D electronic DOS. It was also reported in this work that the shape of the Raman band associated with the tangential modes (between $1500\text{--}1600 \text{ cm}^{-1}$) obtained with the la-

ser energy $E_{\text{laser}} = 1.92 \text{ eV}$ was qualitatively different from those recorded with either higher or lower E_{laser} . Kasuya *et al.*³ recently reported a similar result for a SWNT sample prepared by the arc discharge method. They observed anomalies in the intensity of the Raman bands and a dip in the optical transmittance spectrum near 1.8 eV, and discussed their results in terms of the existence of critical points (singularities) in the electronic DOS of carbon nanotubes.

In a previous resonant Raman study of SWNTs,⁴ we suggested that the change in the shape of the tangential Raman band obtained for $E_{\text{laser}} = 1.92 \text{ eV}$ could be related to the optical transitions of the metallic nanotubes. We present here a detailed experimental study and a consistent explanation for the special resonance Raman scattering behavior of the high-frequency tangential displacement modes of SWNTs in the critical region between 1.7 and 2.2 eV. It is shown here how the spectra change from the relatively sharp bands observed for low and high energy laser lines to the broad bands observed for $1.7 \text{ eV} \leq E_{\text{laser}} \leq 2.2 \text{ eV}$. The dependence of the relative intensity of the enhanced peaks as a function of E_{laser} is explained using a theoretical expression for the Raman cross section that takes into account the distribution of metallic nanotubes in the sample.

The SWNT sample was synthesized by the group at Rice University using the laser vaporization of a carbon target

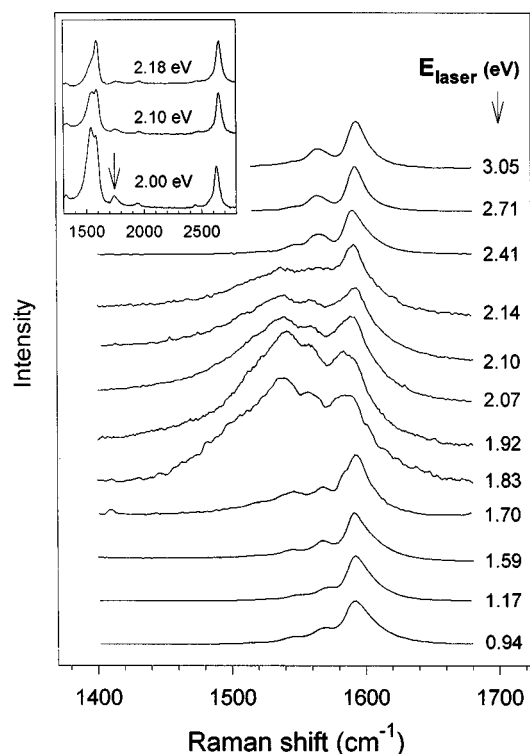


FIG. 1. Raman spectra of the tangential modes of carbon nanotubes obtained with several different laser lines. The inset shows low-resolution Raman spectra between 1300 and 2800 cm^{-1} in the critical range of laser energies 2.00–2.18 eV.

containing 1 to 2 atom % of Ni/Co catalyst in a furnace at 1200 $^{\circ}\text{C}$.^{2,7} The diameter distribution obtained from the TEM contrast image is centered at $d_0 = 1.37$ nm and the full width of the distribution is $\Delta d = 0.18$ nm. Raman scattering experiments were performed at ambient conditions using different experimental setups, in a back-scattering geometry for the following laser excitation lines: krypton 406.7, 647.1, and 676.4 nm (3.05, 1.92, and 1.83 eV); argon 457.9, 488, and 514.5 nm (2.71, 2.54, and 2.41 eV); dye laser 620–570 nm (2.00–2.18 eV); Ti-sapphire 730 nm (1.70 eV); $\text{Al}_x\text{Ga}_{1-x}\text{As}$ diode 780 nm (1.59 eV); and Nd:YAG 1320 and 1064 nm (0.94 and 1.17 eV).

Figure 1 shows the Raman band associated with the tangential C-C stretching modes of the SWNTs, obtained with different laser lines over a wide energy range ($0.94 \leq E_{\text{laser}} \leq 3.05$ eV). Note that the spectra obtained for $E_{\text{laser}} < 1.7$ eV or $E_{\text{laser}} > 2.2$ eV are quite similar, and each spectrum is dominated by a peak at 1593 cm^{-1} . It is important that all of these spectra can be fit by essentially the same set of Lorentzians. Tentative assignments of the individual peaks that compose these bands are given in Refs. 2, 4, and 8. In contrast, the spectra obtained in the narrow range $1.7 \leq E_{\text{laser}} \leq 2.2$ eV are qualitatively different; the bands are broader and centered at lower frequencies.

The inset of Fig. 1 shows low-resolution Raman spectra between 1300 and 2800 cm^{-1} using three laser energies in the transition region between the two regimes. The three spectra were collected using the same experimental conditions, and the most prominent features are the tangential band in the 1500–1600 cm^{-1} range and a second-order band around 2700 cm^{-1} .⁹ The intensity of the second-order band

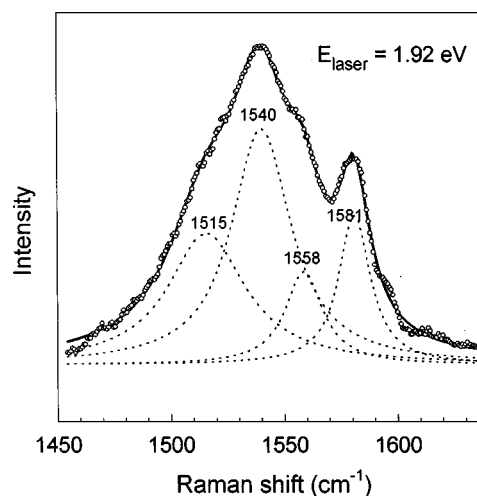


FIG. 2. Raman band associated with the tangential modes of carbon nanotubes for $E_{\text{laser}} = 1.92$ eV obtained by subtracting the basic curve that fits bands obtained in the ranges $E_{\text{laser}} < 1.7$ eV and $E_{\text{laser}} > 2.2$ eV. The dotted curves represent the four specially enhanced Lorentzian peaks. The solid curve corresponds to the fit to the deconvolved experimental data (open circles).

at 2700 cm^{-1} is almost independent of E_{laser} in this range of energies, whereas the intensity of the tangential band is enhanced when E_{laser} approaches 2 eV. It is interesting that the intensity of the faint Raman peak at ≈ 1750 cm^{-1} (indicated by a small arrow in the inset of Fig. 1) also increases in the region of laser energies 1.7–2.2 eV. This peak is associated with a second-order Raman process involving the combination of the radial breathing mode (RBM) around 180 cm^{-1} and the tangential modes between 1500–1600 cm^{-1} . The RBM is uniquely observed in the Raman spectra of single-wall carbon nanotubes, and therefore the presence of this second-order Raman peak is a signature of SWNTs. Since the increase in the intensity of the 1750 cm^{-1} peak accompanies the enhancement of modes between 1500–1600 cm^{-1} in the critical region of laser energies 1.7–2.2 eV, we conclude that the special enhancement of the tangential band is a phenomenon intrinsically related to SWNTs.

Figure 1 shows that, by decreasing the laser energy from 3 to 1 eV, a broad band appears at about 2.2 eV, reaches a maximum intensity around 1.9 eV (red light), and disappears below 1.7 eV. To highlight the part of the tangential Raman band that is specially enhanced in the red, we first subtract the basic spectral band that appears in all the spectra obtained for $E_{\text{laser}} < 1.7$ eV or $E_{\text{laser}} > 2.2$ eV. Figure 2 shows the resulting deconvoluted Raman band for $E_{\text{laser}} = 1.92$ eV. Note that this band can be fit by four Lorentzian peaks at 1515, 1540, 1558, and 1581 cm^{-1} , which are represented by the dotted curves. All Raman bands in this critical region of laser energies (1.7–2.2 eV) can be analyzed in a similar way, and the subtracted spectra can always be fit using the same set of frequencies and relative intensities.

To investigate the laser energy dependence of the specially enhanced peaks in Fig. 2, we tried to calibrate the SWNT Raman spectra by also recording the spectra of silicon and benzoic acid, using the same experimental conditions. However, the results of such calibration were not consistent and reproducible, since the intensity of the SWNT

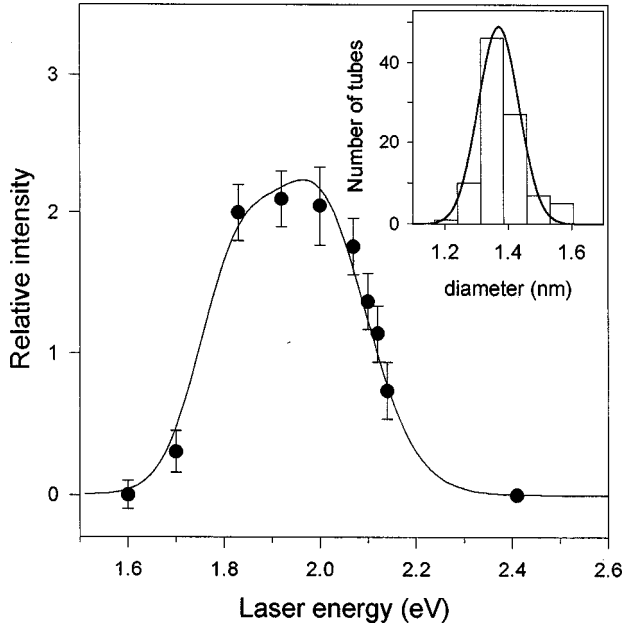


FIG. 3. The solid circles represent the intensity ratio of the Raman peaks at 1540 and 1593 cm^{-1} , and the solid curve represents the fit to the experimental data using Eqs. (1) and (2). The inset shows the distribution of diameters measured by TEM² and the Gaussian fit to the diameter distribution data.

spectrum is strongly dependent on the position of the laser beam in the sample (noting that our data have been obtained in different experimental setups and using different laser sources). Therefore, we also used an internal calibration reference, namely the intensity of the 1593 cm^{-1} peak, since it is present in all SWNT spectra and is the most intense line observed outside the critical region $1.7\text{--}2.2\text{ eV}$. To represent the dependence of the intensity of the enhanced peaks (dotted peaks in Fig. 2) on E_{laser} , we plot in Fig. 3 (solid circles) the ratio of the intensities of the peaks at 1540 cm^{-1} and 1593 cm^{-1} , I_{1540}/I_{1593} . We used the 1540 cm^{-1} peak because it is the most prominent feature of the red enhanced Raman band, but similar results are obtained for Fig. 3 if we use any one of the other three dotted peaks in Fig. 2, except for a change in the normalization factor of the vertical axis scale in Fig. 3. It must be mentioned that the intensity of the 1593 cm^{-1} peak might also depend on laser energy. However, the fact that we obtained excellent agreement between the laser energy dependence of I_{1540}/I_{1593} with the model that is presented in the following discussion shows that the intensity of the 1593 cm^{-1} peak does not depend significantly on E_{laser} in this narrow energy range ($1.7\text{--}2.2\text{ eV}$).

It is well known that the structures of the 1D electronic DOS for the metallic and the semiconducting nanotubes are fundamentally different. According to theoretical^{9–12} calculations, which have been recently confirmed by scanning tunneling microscopy and spectroscopy (STM and STS) experiments^{13,14} on SWNTs, the electronic DOS for semiconducting SWNTs exhibits a larger number of singularities close to the Fermi level than for the metallic nanotubes. These STS experiments^{13,14} showed that within each tube category (metallic or semiconducting), the electronic DOS is practically independent of the chirality of the tube. This re-

sult is consistent with recent calculations^{11,12} showing that the energy separation between the 1D DOS singularities in the valence and conduction bands is proportional to $1/d$, but that the number of singularities is approximately two times greater for semiconducting tubes than for metallic tubes. The STS experiments by the Delft group¹³ were done on samples⁷ very similar to the sample used in our experiments, and show that the metallic nanotubes exhibit an energy separation ($E_{11} = E_{c_1} - E_{v_1}$) between the first pair of DOS singularities in the valence (v) and conduction (c) bands in the range of energy $1.7\text{--}2.0\text{ eV}$, whereas the semiconducting SWNTs exhibit an electronic energy gap (E_{11}) between $0.5\text{--}0.65\text{ eV}$, much lower in energy.

Let us consider now the resonant enhancement of the Raman modes associated with the transitions between DOS singularities for the metallic nanotubes. We first note the similarity between the range of energy separations for the metallic nanotubes measured directly by STS ($1.7\text{--}2.0\text{ eV}$) and the range of laser energies associated with the specially enhanced modes in the Raman spectra ($1.7\text{ eV} \leq E_{\text{laser}} \leq 2.2\text{ eV}$). In our analysis of the Raman spectra, we consider only the $v_1 \rightarrow c_1$ transition, since the energy separation $E_{22} = E_{c_2} - E_{v_2}$ is always greater than 3 eV for the tubes present in our sample, and the optical transitions $v_1 \rightarrow c_2$ and $v_2 \rightarrow c_1$ involve, in general, electronic states with different wave vectors and therefore occur with smaller probability.⁶ For a metallic tube with a given diameter d , the enhancement of its Raman peaks will occur whenever the incident or scattered photon is in resonance with $E_{11}(d) = E_{c_1}(d) - E_{v_1}(d)$.⁶ Considering that our sample contains several types of metallic nanotubes with diameters in the range $1.1\text{--}1.6\text{ nm}$ and that the distribution of diameters for the metallic nanotubes follows the same Gaussian distribution as all the nanotubes (see inset of Fig. 3), the overall enhancement of the intensity of the Raman modes is given by the sum of the contributions of each individual nanotube with a given diameter d , weighted by the distribution of diameters. The Raman cross section $I(E_{\text{laser}})$ can then be written as

$$I(E_{\text{laser}}) = \sum_{d=1.1\text{ nm}}^{1.6\text{ nm}} A \exp\left[-\frac{(d-d_0)^2}{\Delta d^2/4}\right] \times [(E_{11}(d) - E_{\text{laser}})^2 + \gamma_e^2/4]^{-1} \times [(E_{11}(d) - E_{\text{laser}} + E_{\text{phonon}})^2 + \gamma_e^2/4]^{-1}, \quad (1)$$

where d_0 and Δd are the center and the width of the Gaussian distribution of diameters (see TEM measurements in the inset to Fig. 3) and E_{phonon} is the average energy (0.197 eV) of the tangential phonons. The damping factor γ_e avoids the divergence of the double resonance expression for the Raman cross section^{6,15} and accounts for the width of the singularities in the electronic DOS and the lifetime of the excited state. For the diameter dependence of E_{11} , we use the expression calculated by White and Todorov,¹¹ and Charlier and Lambin,¹²

$$E_{11}(d) = \frac{6ac_c\gamma_0}{d}, \quad (2)$$

where a_{C-C} is the carbon-carbon distance and γ_0 is the electronic overlap integral.

The determination of the Raman cross section as a function of E_{laser} involves only three adjustable parameters: the damping factor γ_e , the arbitrary normalization factor A , and γ_0 occurring in Eq. (2). The solid curve in Fig. 3 corresponds to the best fit to the I_{1540}/I_{1593} vs E_{laser} data, and the relevant fitting parameters were found to be $\gamma_0 = 2.95 \pm 0.05$ eV and $\gamma_e = 0.04 \pm 0.02$ eV. The value obtained for γ_e is quite reasonable for the width of a DOS singularity.¹³ The mean value for energy separation $\langle E_{11} \rangle$ and the full width of the distribution ΔE_{11} obtained from Eq. (2) for ($\gamma_0 = 2.95$ eV, $d_0 = 1.37$ nm and $\Delta d = 0.18$ nm) are $\langle E_{11} \rangle = 1.84$ eV and $\Delta E_{11} = 0.24$ eV, which are also in good agreement with the direct measurements of E_{11} by STS.¹³

The excellent fit of the laser energy dependence of the relative intensity of the specially enhanced modes by the Raman cross-section expression for the metallic nanotubes [Eq. (1)] and the good agreement between our results and the direct measurements of the energy separation E_{11} by STS allow us to conclude that the Raman modes specially enhanced in the laser energy range 1.7–2.2 eV are associated with metallic nanotubes. Our results are also in agreement with a recent Electron Energy Loss Spectroscopy (EELS)

experiment,¹⁶ which shows a feature at 1.8 eV in the optical conductivity that originates from the metallic nanotubes.

A last remark concerns the physical origin of the specially enhanced tangential Raman modes. As already discussed, these modes are downshifted and broadened compared to those present in all spectra for E_{laser} between 1 and 3 eV. Frequency shifts and line-shape changes occur in many systems that exhibit strong electron-phonon coupling.^{15,17} In the present case, these changes may be due to renormalization effects associated with the coupling between the phonons and the conduction electrons in the metallic nanotubes. The precise nature of the coupling remains an open question.

The authors gratefully acknowledge valuable discussions with Dr. R. Saito, Dr. J.-C. Charlier, and Dr. C. Dekker. One of us (M.A.P.) is thankful to the Brazilian agency CAPES for financial support during his visit to MIT, and A.M. gratefully acknowledges support from the NATO-CNR. The MIT authors acknowledge support for this work under NSF Grant No. DMR 98-04734 and the U.K. authors acknowledge NSF Grant No. OSR-94-52895. The measurements performed at the George R. Harrison Spectroscopy Laboratory at MIT were supported by NIH Grant No. P41-RR02594 and NSF Grant No. CHE9708265.

*Permanent address: Departamento de Física, Universidade Federal de Minas Gerais, Belo Horizonte, 30123-970 Brazil. Electronic address: mpimenta@fisica.ufmg.br

¹J. Kastner, T. Pichler, H. Kuzmany, S. Curran, W. Blau, D. N. Weldon, M. Dlamasiere, S. Draper, and H. Zandbergen, *Chem. Phys. Lett.* **221**, 53 (1994).

²A. M. Rao, E. Richter, S. Bandow, B. Chase, P. C. Eklund, K. W. Williams, M. Menon, K. R. Subbaswamy, A. Thess, R. E. Smalley, G. Dresselhaus, and M. S. Dresselhaus, *Science* **275**, 187 (1997).

³A. Kasuya, M. Sugano, Y. Sasaki, T. Maeda, Y. Saito, K. Tohji, H. Takahashi, Y. Sasaki, M. Fukushima, Y. Nishina, and C. Horie, *Phys. Rev. B* **57**, 4999 (1998).

⁴M. A. Pimenta, A. Marucci, S. D. M. Brown, M. J. Matthews, A. M. Rao, P. C. Eklund, R. E. Smalley, G. Dresselhaus, and M. S. Dresselhaus, *J. Mater. Res.* **13**, 2396 (1998).

⁵M. Sugano, A. Kasuya, Y. Sasaki, K. Tohji, Y. Saito, and Y. Nishina, *Chem. Phys. Lett.* **292**, 575 (1998).

⁶E. Richter and K. R. Subbaswamy, *Phys. Rev. Lett.* **79**, 2738 (1997).

⁷A. Thess, R. Lee, P. Nikolaev, H. Dai, P. Petit, J. Robert, C. Xu, Y. H. Lee, S. G. Kim, A. G. Rinzler, D. T. Colbert, G. E.

Scuseria, D. Tománek, J. E. Fischer, and R. E. Smalley, *Science* **273**, 483 (1996).

⁸A. Kasuya, Y. Sasaki, Y. Saito, K. Tohji, and Y. Nishina, *Phys. Rev. Lett.* **78**, 4434 (1997).

⁹M. S. Dresselhaus, G. Dresselhaus, and P. C. Eklund, *Science of Fullerenes and Carbon Nanotubes* (Academic Press, New York, 1996).

¹⁰R. Saito, G. Dresselhaus, and M. S. Dresselhaus, *Physical Properties of Carbon Nanotubes* (Imperial College Press, London, 1998).

¹¹C. T. White and T. N. Todorov, *Nature (London)* **393**, 240 (1998).

¹²J. C. Charlier and Ph. Lambin, *Phys. Rev. B* **57**, R15 037 (1998).

¹³J. W. G. Wildöer, L. C. Venema, A. G. Rinzler, R. E. Smalley, and C. Dekker, *Nature (London)* **391**, 59 (1998).

¹⁴T. W. Odom, J. L. Huang, P. Kim, and C. M. Lieber, *Nature (London)* **391**, 62 (1998).

¹⁵A. S. Barker and R. Loudon, *Rev. Mod. Phys.* **44**, 18 (1972).

¹⁶T. Pichler, M. Knupfer, M. S. Golden, J. Fink, A. Rinzler, and R. E. Smalley, *Phys. Rev. Lett.* **80**, 4729 (1998).

¹⁷P. Eklund and K. R. Subbaswamy, *Phys. Rev. B* **20**, 5157 (1979).